

Direct Measurement of Plasma Space Potential on Elmo Bumpy Torus

P. L. Colestock, K. A. Connor, and R. L. Hickok

Department of Electrical and Systems Engineering, Rensselaer Polytechnic Institute, Troy, New York 12181

and

R. A. Dandl

Fusion Energy Division, Oak Ridge National Laboratory, Oak Ridge, Tennessee 37830

(Received 9 January 1978)

A heavy-ion-beam probe has been used to measure the space-potential distribution on the Elmo bumpy torus. The results indicate that under optimum confinement conditions the ambipolar electric field is nearly axisymmetric, points radially inward, and is of sufficient magnitude to dominate the ion poloidal drifts.

The Elmo bumpy torus at Oak Ridge National Laboratory is a plasma-confinement experiment which utilizes microwave heating in a set of toroidally connected magnetic mirrors. The spatial periodicity of the magnetic field results in ∇B and curvature drifts which average out the toroidal drift while microwave-driven electron-plasma ring currents produce an average minimum- B configuration for overall MHD (magneto-hydrodynamic) stability.¹ In such a device the ambipolar electric field is of critical importance.² If E is large enough, both positive- and negative-particle drifts will be dominated by $\vec{E} \times \vec{B}$. In this Letter we discuss an experimental study of the radial potential distribution in the Elmo bumpy torus that shows the role played by the $\vec{E} \times \vec{B}$ drift.

A heavy-ion-beam probe³⁻⁵ has been used to measure directly the ambipolar potential in the midplane of a single mirror section. A schematic representation of the ion-beam probe is shown in Fig. 1. A singly ionized 8-30-kV rubidium beam (primary) is injected in the midplane producing a spray of doubly charged rubidium ions (secondaries) by electron-impact collisions. The secondaries are separated from the primary

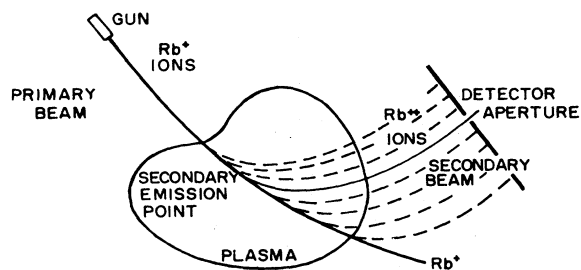


FIG. 1. Schematic representation of the beam-probing experiment. Singly charged rubidium ions are injected into the plasma and doubly charged ions are produced by electron-impact collisions.

beam by the magnetic field. The change in charge state of the secondaries causes them to leave the plasma with an additional amount of energy exactly equal, in volts, to the plasma space potential at the point of secondary ionization.

A small-aperture electrostatic energy analyzer, located in the field-free region outside the plasma, measures the energy (to within 5 V) of the secondaries produced in a small volume (about 1 cm³) of the ion beam. This sensitivity is obtained by chopping the beam and using synchronous detection.⁶ The sample volume can theoretically be moved anywhere in the minor cross section of the plasma by varying the beam energy and injection angle. However, as set up, the beam probe could fully scan only the lower half of the plasma and a small part of the upper half.

The space-potential profile along the horizontal axis (cf. Fig. 2) with the device operating in the C mode (collisional mode—low stored energy and

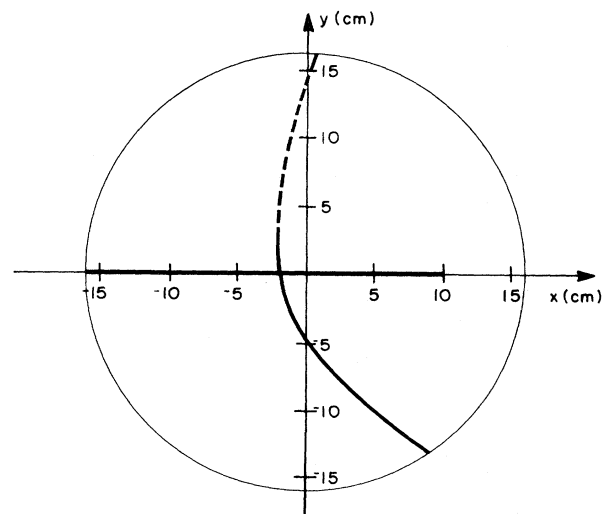


FIG. 2. Horizontal and vertical scan lines referenced to cavity coordinates. Cavity radius is 20 cm.

electron temperature) is shown in Fig. 3(a). The potential is slightly positive in the center and is slightly peaked on the inside of the torus. The ambipolar field is relatively low with a peak potential difference of about 75 V. A corresponding profile taken along the vertical curve of Fig. 2 is shown in Fig. 3(b). The results are qualitatively the same as for the horizontal profile. The vertical curve of Fig. 2 and other scans of the same type, but displaced to the right or left, show vertical symmetry where the beam probe can measure the potential in the upper half-plane (2–4 cm above the horizontal axis). The two-dimensional profile of Fig. 3(c) is produced by a spline fit to all the data, assuming vertical symmetry to complete the map of the entire cross section. The detailed structure of the profiles has been removed from the figure for clarity. The circular boundary denotes the cross section where the measurements were made while the outer flat surface region is provided for zero reference.

The corresponding results for the T mode

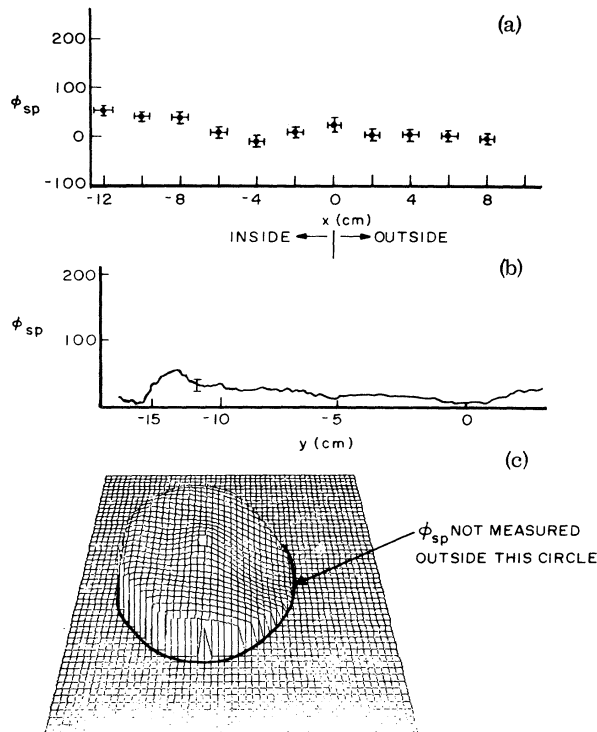


FIG. 3. Space-potential scans in the C mode. (a) Horizontal profile centered on cavity axis. (b) Vertical profile of Fig. 2. (c) Two-dimensional potential map generated assuming vertical symmetry and using a spline fit to the data.

(toroidal mode—high stored energy and electron temperature) are shown in Figs. 4(a)–4(c). The potential is strongly peaked on the outside and is nearly axisymmetric, centered at a point located approximately 4 cm towards the inside, as shown in Fig. 4(a). The maximum potential difference in this case is nearly 200 V. The corresponding vertical profile is shown in Fig. 4(b). The results are similar except that a double peak occurs at $y \approx 13$ cm. This point is further removed from the plasma center than points which are measurable on the horizontal profile; hence the double peak, if it is there, is not observed in the horizontal-profile measurements. The positions of the double peak and the electron ring² both approximately coincide with the resonance layer and consequently move when the magnetic field is varied. The two-dimensional profile is shown in Fig. 4(c) indicating a relatively large, radially-inward-directed ambipolar field.

The profiles for the C and T modes shown in Figs. 3 and 4 are typical, but since the two modes incorporate large classes of operating conditions, they are not unique. The C (collisional) mode, for example, is produced by relatively large neu-

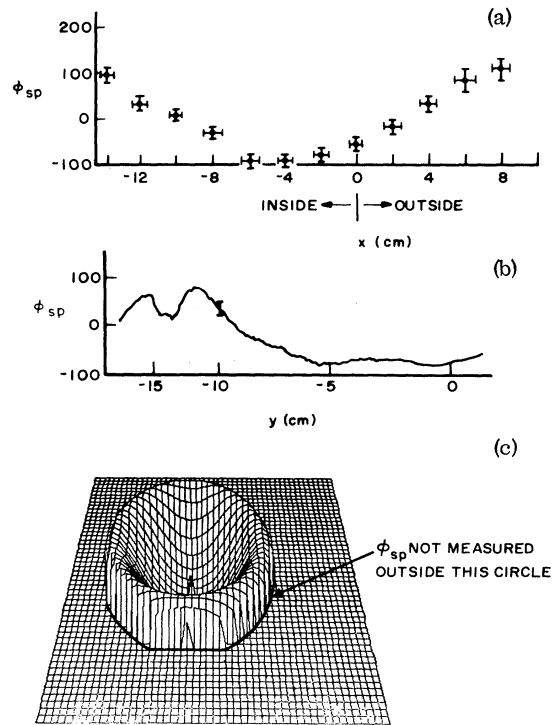


FIG. 4. Space-potential scans in the T mode. Scans correspond to those of Fig. 2. (a) Horizontal profile. (b) Vertical profile of Fig. 2. (c) Two-dimensional potential map.

tral-gas pressures which, if high enough, can be characterized by a potential peak in the center region. As the pressure is reduced the profile passes through that of Fig. 3 and then through a smooth transition (Fig. 5) into the T (toroidal) mode profile of Fig. 4. A series of radial scans along the canted vertical line of Fig. 2 is shown in Fig. 5 for several filling pressures transversing the C-T transition. The change in plasma parameters which denotes the C mode occurs rather abruptly at approximately $P = 1.3 \times 10^{-5}$ Torr. Fluctuation levels, as measured with a microwave interferometer, increase by a factor of 40 and the stored perpendicular energy decreases by a factor of 10 in going from the lowest to highest pressures shown in Fig. 5. The structure of the profiles is reproducible and the transition occurs more gradually than the changes in the plasma temperature, density, and perpendicular energy density.

The most significant result of this study is the fact that the ambipolar field in the T mode is nearly axisymmetric and points radially inward with respect to the plasma axis. Moreover, the size and axisymmetry of the potential profile result in an important contribution to the poloidal drifts that are necessary to average out the drift produced by the toroidal character of the magnetic field. The importance of the contribution may be

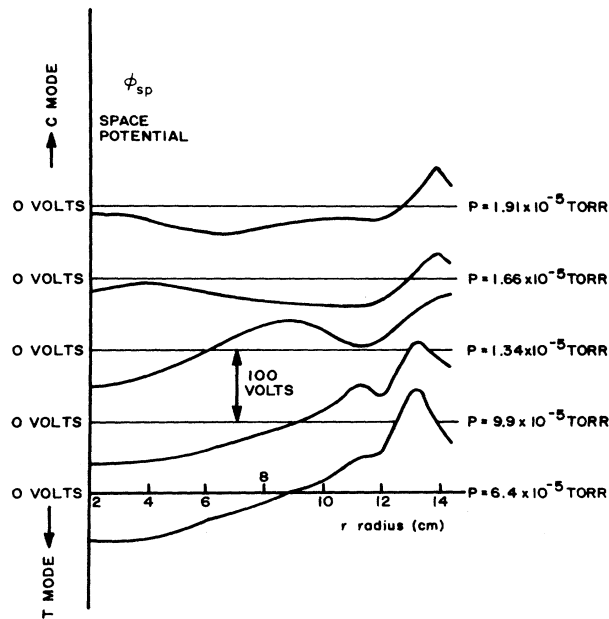


FIG. 5. Space-potential profiles along a canted vertical profile for several pressures near the C-T mode transition. Microwave power is held constant.

assessed by comparing the various drifts associated with single-particle orbits in electric and magnetic fields.⁷ The curvature-drift frequency for species α is $kT_{\alpha}/q_{\alpha}BR_C a$, and the $\vec{E} \times \vec{B}$ drift frequency is E/Ba , where R_C is the mirror radius of curvature and a is the minor radius. Since E points inward, the drifts add for electrons and subtract for ions. In general, for particles whose energy is less than $q\phi_{\max}$ the $\vec{E} \times \vec{B}$ drift dominates the curvature drifts, where ϕ_{\max} is the potential well depth. In the T mode, $q\phi_{\max}/kT_i \approx 2$ so that the ion distribution is dominated by the $\vec{E} \times \vec{B}$ drift while the drift of the bulk of the electron distribution ($q\phi_{\max}/kT_e \approx 1$) is increased by this term. The resulting increase in drift frequency reduces the loss rate.⁸

The electric field enhances confinement for both species of particles, however an additional ion-loss effect occurs that equalizes the two loss rates. If there were no electric field, the electrons would be lost faster than the ions. The buildup of the electric field causes a small class of ions in the tail of the distribution to diffuse more rapidly because the $\vec{E} \times \vec{B}$ drift cancels the ∇B drift for these particles. The increased loss rate is due to the super banana orbits that result when the ion experiences no poloidal drift at some point. A self-consistent electric field exists within this loss is sufficient to balance with the electrons. It is clear then that the model for neoclassical transport for plasma parameter scaling of this confinement scheme must include the electric field in a self-consistent manner if it is to provide an accurate picture of the physics of Elmo bumpy torus.⁹

This work was supported by the Union Carbide Corporation, Nuclear Division, under Contract No. Sub 7044.

¹R. A. Dandl, H. O. Eason, G. E. Guest, C. L. Hedrick, H. Ikegami, and D. B. Nelson, in *Proceedings of the Fifth International Conference on Plasma Physics and Controlled Nuclear Fusion Research, Tokyo, Japan, 1974* (International Atomic Energy Agency, Vienna, Austria, 1975), Vol. II, p. 141.

²R. A. Dandl *et al.*, ORNL Report No. ORNL-TM-4941, 1975 (unpublished).

³F. C. Jobes and R. L. Hickok, *Nucl. Fusion* **10**, 195 (1970).

⁴J. C. Hosea, F. C. Jobes, R. L. Hickok, and A. N. Dellis, *Phys. Rev. Lett.* **30**, 839 (1973).

⁵R. E. Reinovsky, J. C. Glowienka, A. E. Seaver,

W. C. Jennings, and R. L. Hickok, IEEE Trans. Plasma Sci. **2**, 250 (1974).

⁶P. Colestock *et al.*, in Proceedings of the Fourth IEEE Conference on Plasma Science, Troy, New York, 1977 (unpublished).

⁷T. G. Northrup, *The Adiabatic Motion of Charged Particles* (Wiley, New York, 1963).

⁸C. L. Hedrick *et al.*, ORNL Report No. ORNL-TM-5490, 1977 (unpublished).

⁹E. F. Jaeger *et al.*, Phys. Rev. Lett. **40**, 866 (1978).

Nonlinear Diffusion Problem Arising in Plasma Physics

James G. Berryman^(a) and Charles J. Holland^(b)

Courant Institute of Mathematical Sciences, New York University, New York, New York 10012

(Received 17 March 1978)

In earlier studies of plasma diffusion with Okuda-Dawson scaling ($D \sim n^{-1/2}$), perturbation theory indicated that arbitrary initial data should evolve rapidly toward the separable solution of the relevant nonlinear diffusion equation. Now a Lyapunov functional has been found which is strictly decreasing in time and bounded below. The rigorous proof that arbitrary initial data evolve toward the separable solution is summarized. Rigorous bounds on the decay time are also presented.

Anomalous diffusion of hydrogen plasma across a purely poloidal octupole magnetic field has been observed experimentally¹ for densities $n_e \sim 5 \times 10^9 \text{ cm}^{-3}$ and poloidal fields B_p in the range 250 G–1 kG. The diffusion coefficient for this anomalous diffusion scales like $D \sim n^{-1/2}$ with D being independent of B_p . This scaling was predicted for vortex diffusion by Okuda and Dawson² when the ratio of ion plasma frequency and ion cyclotron frequency satisfies $\Omega_{pi}^2/\Omega_{ci}^2 \gg 1$, and was first observed by Tamano, Prater, and Ohkawa.³ The Wisconsin octupole experiments have shown that after a few milliseconds the density profile evolves into a fixed shape (the "normal mode") which then decays in time. Numerical studies¹ indicated that the normal mode shape was well approximated by the shape of the separable solution of the relevant one-dimensional diffusion equation.

In normalized units, the diffusion equation may be written as^{4,5}

$$\frac{\partial}{\partial x} \left[D(n) \frac{\partial n}{\partial x} \right] = F(x) \frac{\partial n}{\partial t} \text{ for } 0 \leq x \leq 1, \quad (1)$$

where x is the spatial variable corresponding to magnetic field potential and t is the time. The geometrical factor $F(x)$ is a positive function determined by the octupole geometry and in general $D(n) \propto n^\delta$ where $\delta \geq -1$. It is convenient to rewrite this equation as

$$u_{xx} = F(x)(u^{q-1})_t, \quad (2)$$

where $q = (2 + \delta)/(1 + \delta)$ and $n = u^{q-1}$. By use of a

perturbation analysis, it was established that the separable solution of (2) is stable against small perturbations. If the separable solution is written as $u(x, t) = S(x)T(t)$, then for $F(x) = \text{const}$ all perturbations decay at least as fast as $T^4(t)$.

In this Letter, we report the first rigorous results on this novel nonlinear diffusion problem. Methods have now been developed to prove that an arbitrary initial density profile will evolve toward the separable solution for $2 < q < \infty$ ($0 > \delta > -1$). To save space, the methods will be illustrated on the model diffusion equation

$$u_{xx}(x, t) = 2u(x, t)u_t(x, t), \quad (3)$$

with $u(0, t) = u(1, t) = 0$, since this corresponds to one case of experimental interest. All the arguments presented here may be generalized for all $2 < q < \infty$. When $F(x) = \text{const}$, the generalization enjoys full mathematical rigor.⁶ When $F(x)$ is an arbitrary positive integrable function, the generalization may at least be carried through formally.⁷

Sabinina⁸ has established the existence and uniqueness of the solutions of (3). She has also shown that a finite time t^* exists when the solution first vanishes identically. We call this time t^* the extinction time.

The proof that arbitrary initial data evolve toward the separable solution will now be summarized. First, introduce the function

$$w(x, t) = u(x, t)/(t^* - t), \quad (4)$$